

Hierarchical confinement achieving cascade phosphorescence resonance energy transfer and application

Jie Yu , Jiuying Liao , Yan Zhao , Yu Liu

PII: S1001-8417(25)01142-8
DOI: <https://doi.org/10.1016/j.ccllet.2025.111964>
Reference: CCLET 111964



To appear in: *Chinese Chemical Letters*

Received date: 23 June 2025
Revised date: 1 October 2025
Accepted date: 13 October 2025

Please cite this article as: Jie Yu , Jiuying Liao , Yan Zhao , Yu Liu , Hierarchical confinement achieving cascade phosphorescence resonance energy transfer and application, *Chinese Chemical Letters* (2025), doi: <https://doi.org/10.1016/j.ccllet.2025.111964>

This is a PDF file of an article that has undergone enhancements after acceptance, such as the addition of a cover page and metadata, and formatting for readability, but it is not yet the definitive version of record. This version will undergo additional copyediting, typesetting and review before it is published in its final form, but we are providing this version to give early visibility of the article. Please note that, during the production process, errors may be discovered which could affect the content, and all legal disclaimers that apply to the journal pertain.

© 2025 Published by Elsevier B.V. on behalf of Chinese Chemical Society and Institute of Materia Medica, Chinese Academy of Medical Sciences.

Communication

Hierarchical confinement achieving cascade phosphorescence resonance energy transfer and application

Jie Yu,^a Jiuying Liao,^a Yan Zhao,^{a,*} Yu Liu^{b,*}^a College of Chemistry and Chemical Engineering, Yunnan Key Laboratory of Modern Separation Analysis and Substance Transformation, Yunnan Normal University, Kunming 650500, China^b College of Chemistry, State Key Laboratory of Elemento-Organic Chemistry, Nankai University, Tianjin 300071, China

ARTICLE INFO

ABSTRACT

*Article history:*Received
Received in revised form
Accepted
Available online*The Keywords:*Cucurbituril
Supramolecular organic framework
Phosphorescence
Supramolecular assembly
Energy transfer

Herein, we report morphology and luminescence tunable supramolecule containing tetracation hexabromoisoquinoline modified tetraphenylbenzene (TQ), cucurbit[8]uril (CB[8]), β -cyclodextrin grafted hyaluronic acid (HACD), and two dyes (SR101, Cy5), which can lead to cascade efficient phosphorescence resonance energy transfer (PRET) through multi-scale supramolecular space confinement to achieve long-lived multi-wavelength emission, especially near-infrared (NIR) luminescence. The initial unit TQ was assembled to form a green phosphorescent 3D supramolecular organic framework (SOF) under the activation of CB[8] confinement and then co-assembled with polysaccharide HACD to form phosphorescence extended long-lifetime (670.3 μ s) 3D nanoparticles. This hierarchical confinement boosted phosphorescence supramolecule can act as the donor to achieve efficient energy transfer from phosphor to the dye SR101, giving long-lived luminescence at 615 nm, which can be employed as a transit depot and further encapsulate secondary acceptor Cy5, achieving efficient delayed NIR fluorescence at 680 nm, and was used as phosphorescence logic gate and NIR imaging reagent.

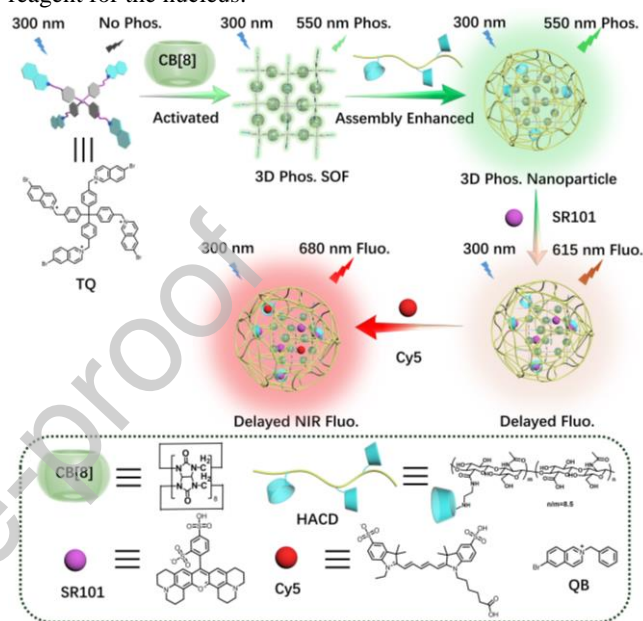
*Corresponding authors.

E-mail addresses: zhaoyann@163.com (Y. Zhao); yuliu@nankai.edu.cn (Y. Liu)

Recently, phosphorescent materials based on macrocyclic compounds have become a research hotspot in chemistry and materials, which were successfully applied in bioimaging [1], hydrogel [2], sensing detection [3], information security [4], and reaction catalysis [5]. In many macrocyclic compounds, cyclodextrin and cucurbit[*n*]uril (CB[*n*], *n* = 6,7,8) have unique advantages in the construction of water soluble supramolecular phosphorescence materials, because they have hydrophobic cavities that can effectively encapsulate luminescent groups through non-covalent interactions such as hydrophobicity, hydrogen bond, and electrostatics [6-9] to prevent collision of solvent molecules and reduce the vibration and rotation of the chromophores, providing confined microenvironment for the phosphorescent groups, thereby promoting its luminescent properties. For example, George *et al.* reported that cationic bromonaphthalimide was encapsulated by CB[7] and further induced blue phosphorescence with a high quantum yield (QY) of up to 41.8% in water [10]. Li *et al.* found that β -cyclodextrin can encapsulate biphenylboronic acid derivatives through host-guest and hydrogen bonding interactions and then assemble to give a green phosphorescence supramolecular system with a long lifetime of 1.03 s in the aqueous phase, which was further applied in energy transfer systems [11]. The Liu group found that CB[8] could encapsulate anthracene-modified bromophenylpyridinium derivative and assemble to form red fluorescence nanofibers that could target the nucleus, which was photooxidized to give green phosphorescent ternary supramolecular complexes with lysosomal targeting ability, realizing photooxidation-driven dual-targeted organelles imaging [12]. Especially, the rigid macrocyclic CB[8] with a large hydrophobic cavity could bind two guest molecules and was used as the supramolecular cross-linker to assemble with cationic arms modified planar or spatial building blocks to give water-soluble 2D or 3D luminescent supramolecular organic frameworks (SOFs) [13-15]. For instance, Cao *et al.* synthesized tetracationic coumarin-modified hexabenzene and assembled with CB[8] to form 2D network fluorescence SOF, which further encapsulates chiral dipeptides to achieve chirality transfer from the guest to SOF, giving induced adaptive circularly polarized luminescence [16]. Recently, Ma *et al.* reported 3D phosphorescence SOF assembled by tetracationic bromophenylpyridinium and CB[8], which can sense antibiotics and adsorb dyes to form the energy transfer system [17]. Although there are some reports on luminescent SOFs, the phosphorescence of 3D SOF is activated and enhanced by the hierarchical confinement of macrocycle and assembly, and then acts as a donor in the cascade energy transfer system to form luminescent properties and morphology controllable supramolecule, which is still rarely reported.

In this work, we report an efficient cascade phosphorescence energy transfer supramolecule with tunable assembly morphology and luminescence achieved by the hierarchical confinement of macrocyclic CB[8] and anionic polysaccharide (Scheme 1). Firstly, the tetracationic hexabromoisoquinoline-modified tetraphenylbenzene (TQ) was encapsulated by CB[8] in a 1:2 stoichiometric ratio and then assembled into a positively charged nanoblock-like 3D SOF, which was simultaneously activated to generate green phosphorescence at 550 nm. Compared with the simple host-guest complex of monocationic hexabromoisoquinoline and CB[8] (QB)/CB[8], the lifetime of cationic SOF was enhanced 19.5 times and reached up to 167.7

μ s. In particular, the SOF can co-assemble with the polymer HACD to form anionic 3D nanoparticles with further extended phosphorescence properties. Then, SR101 was introduced as the acceptor and encapsulated by the cyclodextrin of HACD and the hydrophobic pore of SOF to achieve the first-stage energy transfer from phosphorescent SOF to the acceptor, giving long-lifetime (101.2 μ s) fluorescence at 615 nm. Furthermore, the cascade energy transfer supramolecule was successfully realized by encapsulating Cy5 as the secondary acceptor, leading to long-lived NIR luminescence at 680 nm. Finally, the controllable supramolecule fabricated by hierarchical confinement can be used as phosphorescent logic gates and the targeted NIR imaging reagent for the nucleus.



Scheme 1. Hierarchical confinement achieving cascade phosphorescence resonance energy transfer.

Firstly, the tetracation guest and compound QB were obtained by the S_N2 substitution reaction of hexabromoisoquinoline with 4-bromomethylphenylbenzene and benzyl bromide, respectively (Scheme S1 in Supporting information). The molecular structure was characterized and confirmed by nuclear magnetic resonance (NMR) and high-resolution mass spectrometry (Figs. S1-S4 in Supporting information). Subsequently, the host-guest properties of guests and CB[8] were studied by UV-vis spectroscopy experiments. In the Job plot of QB/CB[8] (Fig. S5 in Supporting information), the maximum change value of the absorption peak appeared at 0.67, indicating the stoichiometric ratio of CB[8] to QB is 1:2, that is, CB[8] with the large cavity can encapsulate two QBs. In Fig S6 (Supporting information), the absorption peaks of QB at 245, 300, and 338 nm gradually decreased with the increasing CB[8] ratios, which was attributed to the inclusion of cationic guest QB by CB[8]. According to the change of the UV-vis absorption signal of QB at 245 nm, the binding constant between QB and CB[8] was calculated as $1.84 \times 10^{12} \text{ M}^{-2}$ (Fig. S7 in Supporting information). Therefore, taking advantage of the characteristics of CB[8] binding with two cationic guests, CB[8] is suitable as the supramolecular crosslinker for SOF. In the Job plot of the four cationic arms guest-TQ and CB[8] (Fig. S8 in Supporting information), the inflection point is located at 0.33, indicating the stoichiometric ratio between CB[8] and TQ is 2n:1n (n represents the number of repeated units) [18]. The UV-

vis titration experiment showed that the characteristic signal of TQ at 248 nm decreased significantly after the addition of CB[8] (Fig. 1a). According to the change of the absorption intensity at 248 nm, the binding constant between TQ and CB was measured as $8.19 \times 10^{12} \text{ M}^{-2}$ (Fig. 1b), indicating CB[8] can effectively bind with TQ and benefit assembly to form stable supramolecules. The binding mode of TQ/CB[8] was further studied by NMR experiments. In Fig. S9 (Supporting information), the protons of H_{a,b} and H_{d,e} in TQ were upfield shifted in the presence of the host, indicating the isoquinoline ring was encapsulated by the cavity of CB[8] [19]. In the presence of 2.0 equiv. host, the proton signals of isoquinoline units in TQ were broadened, which was attributed to the formation of a large aggregate of SOF [20].

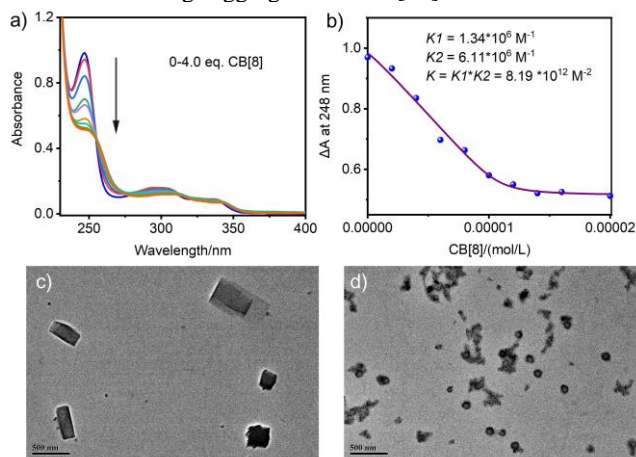


Fig. 1. (a) UV-vis spectra of TQ in the presence of different amounts of CB[8] ([TQ] = 0.05 mmol/L). (b) Nonlinear least-squares analysis of the absorbance intensity changes of TQ in the presence of CB[8] to measure the binding constant (K). TEM images of (c) TQ/CB[8] and (d) TQ/CB[8]/HACD.

The influence of macrocyclic and assembly confinement on the assembly behavior and topological morphology of TQ was investigated by transmission electron microscopy (TEM), dynamic light scattering (DLS), and zeta potential experiments. TEM picture showed that TQ/CB[8] was assembled to form nanoblocks with large sizes in the range of 250–520 nm (Fig. 1c). After secondary assembly with polysaccharide HACD, many irregular nanoparticles were observed in the TEM image of TQ/CB[8]/HACD (Fig. 1d), achieving assembly morphology transferred from 3D nanoblocks to nanoparticles by hierarchical confinements of macrocycle and assembly. In addition, the AFM picture (Fig. S10 in Supporting information) shows that the thickness and aspect ratio of the TQ/CB[8]/HACD were measured as 10.58 nm and 0.22, respectively, confirming the formation of 3D nanoparticles. Furthermore, DLS experiments showed that the average size of SOF was tested as 531 nm with a narrow particle size distribution (Fig. S11 in Supporting information). After the second assembly, the size of the assembly decreased and distributed mainly in two ranges of 30–70 nm and 105–500 nm (Fig. S11), which was basically consistent with the TEM result. In addition, the zeta potential of TQ/CB[8] decreased from +3.03 to -7.52 mV in the presence of HACD (Fig. S12 in Supporting information), further confirming the positively charged SOF transferred to the anionic supramolecule (TQ/CB[8]/HACD) after co-assembly with the polysaccharide.

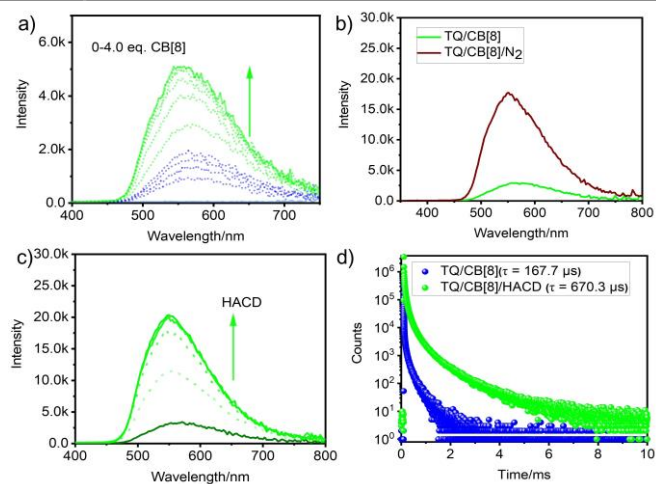


Fig. 2. (a) Phosphorescence spectra of TQ in the presence of CB[8] ([TQ] = 0.02 mmol/L, λ_{ex} = 300 nm, delayed 50 μs). (b) Phosphorescence spectra of TQ/CB[8] bubbled with N_2 ([TQ] = 0.02 mmol/L, λ_{ex} = 300 nm, delayed 50 μs). (c) Phosphorescence spectra of TQ/CB[8] in the presence of HACD (0–0.8 equiv.) ([TQ] = 0.02 mmol/L, [CB[8]] = 0.04 mmol/L, λ_{ex} = 300 nm, delayed 50 μs). (d) Phosphorescence lifetime of TQ/CB[8] and TQ/CB[8]/HACD at 550 nm ([TQ] = 0.02 mmol/L, [CB[8]] = 0.04 mmol/L, [HACD] = 0.012 mmol/L, λ_{ex} = 300 nm).

Phosphorescence spectroscopy experiments were performed to investigate the macrocyclic and assembly confinement activation for the luminescence performance of TQ. In Fig. 2a, no signal was observed for free TQ, and the induced signals emerged at 550 nm with the increase ratio of CB[8]. After being introduced to nitrogen gas, the photoluminescence intensity of TQ/CB[8] increased significantly (Fig. 2b) and the lifetime increased from 167.7 μs to 313.4 μs (Fig. S13 in Supporting information), ascribing to N_2 bubbling reduces dissolved oxygen in water, thereby diminishing its quenching effect on luminophores, confirming that TQ was activated to give 550 nm phosphorescence under the confinement of CB[8] [21,22]. In addition, the monocationic QB was also activated to give phosphorescence under the confinement of CB[8] (Fig. S14 in Supporting information). It is worth noting that the lifetime of SOF was increased by 19.5 times compared with QB/CB[8] (Fig. S15 in Supporting information), which may be because the formation of SOF assemblies is conducive to further confining phosphors and promoting phosphorescence emission. Inspired by this point, the application of the cascade assembly of SOF and HACD may further improve the phosphorescence performance. As shown in Fig. 2c, the phosphorescence intensity of SOF was further increased with the addition of HACD, and the lifetime was cascade enhanced 4 times up to 670.3 μs as well as the quantum yield was increased from 0.27% to 0.94% (Fig. S16 in Supporting information), which was ascribe to the hierarchical assembly could further reduce the movement of the luminescent moieties, significantly prevent the influence of solvent molecules on the luminophores, and then expand its phosphorescence performance. Therefore, multiscale hierarchical confinement can activate and improve the phosphorescence performance of the phosphors in the aqueous phase and promote the luminescence of the SOF.

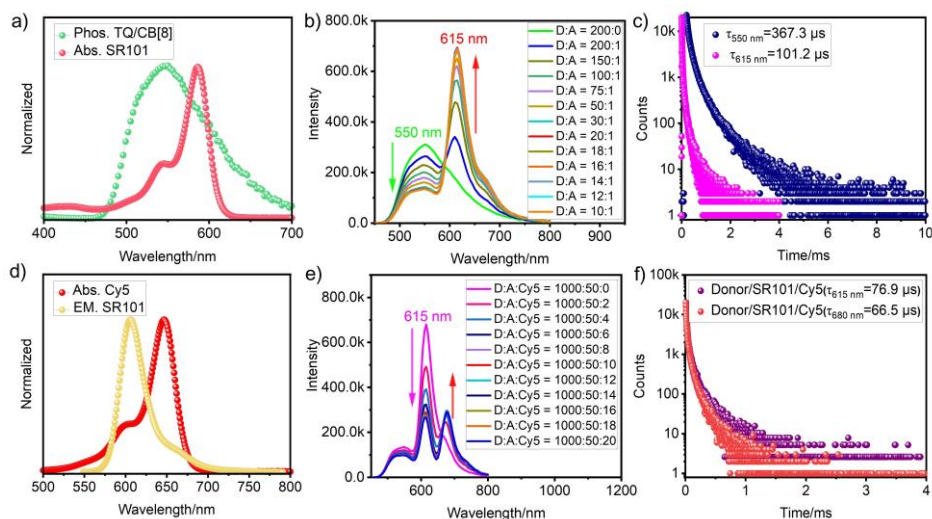


Fig. 3. (a) Normalized phosphorescence spectrum of TQ/CB[8] and absorbance spectrum of SR101. (b) Phosphorescence spectra of TQ/CB[8]/HACD (represented as “D”) in the presence different amounts of SR101 (represented as “A”) ([TQ] = 0.02 mmol/L, [CB[8]] = 0.04 mmol/L, [HACD] = 0.012 mmol/L, λ_{ex} = 300 nm, delayed 50 μs). (c) Phosphorescence lifetime of TQ/CB[8]/HACD/SR101 at 550 nm and 615 nm, respectively. (d) Normalized fluorescence spectrum of SR101 and absorbance spectrum of Cy5. (e) Phosphorescence spectra of TQ/CB[8]/HACD/SR101 in the presence different amounts of Cy5 ([TQ] = 0.02 mmol/L, [CB[8]] = 0.04 mmol/L, [HACD] = 0.012 mmol/L, [SR101] = 0.001 mmol/L, λ_{ex} = 300 nm, delayed 50 μs). (f) Phosphorescence lifetime of TQ/CB[8]/HACD(Donor)/SR101/Cy5 at 615 nm and 680 nm, respectively.

Benefiting from the cascade assembly strategy, the formed aqueous supramolecule not only has good phosphorescence properties, but also has the cavity of cyclodextrin and the assembly pore structure of SOF, which is suitable for loading dyes as acceptors to form a phosphorescence energy transfer system and realize the regulation of luminescence behavior. Fig. 3a shows that the absorption spectrum of SR101 has a good overlap with the phosphorescence spectrum of SOF; thus, SR101 may be used as the acceptor for the energy transfer system [23,24]. When SR101 was added to the phosphorescence supramolecule, the phosphorescence signal of TQ/CB[8]/HACD at 550 nm was decreased, and a new emission peak at 615 nm was observed (Fig. 3b), indicating that the energy was transferred from the excited phosphorescence group to the acceptor dye. The phosphorescence lifetime of the assembly at 550 nm was reduced to 367.3 μs (Fig. 3c), which further confirms the occurrence of first-order energy transfer. According to the change of the intensity of the phosphorescence peak at 550 nm, the energy transfer efficiency was calculated to be 57.4 %. Since the absorption spectrum of Cy5 has a good overlap with the emission peak of SR101, it was selected as a secondary energy acceptor for the cascade energy transfer supramolecule. Fig. 3e shows that with the addition of Cy5 to the first-order energy transfer system, the emission peak at 615 nm gradually decreases, and the signal at 680 nm emerges. The lifetime of the supramolecular system at 615 nm decreased from 101.2 μs to 76.9 μs , and the lifetime at 680 nm was measured to be 66.5 μs (Fig. 3f) after adding Cy5, indicating the occurrence of secondary energy transfer from SR101 to the NIR dye. Quantify energy transfer rates were measured as 1.23×10^3 and 3.12×10^3 s^{-1} , respectively. According to the change of fluorescence signal intensity at 615 nm, the secondary energy transfer efficiency is calculated to be 60.8%. The QY of the fabricated NIR supramolecule was measured to be 10.05% (Fig. S17 in Supporting information). In addition, the single SR101 and Cy5 could not give the emission peaks at 615 nm and 680 nm under the same conditions (Fig. S18 in Supporting formation), confirming hierarchical confinement boosted efficient cascade energy transfer in the supramolecule.

The constructed NIR supramolecular with efficient energy transfer and good luminescent properties may be attributed to the fact that CB[8] encapsulates the TQ as a donor, effectively preventing the phosphorescence quenching caused by molecular collision; on the other hand, the cyclodextrin of HACD can effectively bind with the acceptors-two dyes (Fig. S19 in Supporting information), restricting the vibration/rotation of the acceptors, promoting energy transfer from excited donor to the acceptor, providing a favorable microenvironment for luminescence.

Considering the hierarchically confined supramolecular system has controllable luminescence behavior and possesses the assembly unit-hyaluronic acid with targeting ability for cancer cells [25-27], which may be used as phosphorescence logic gates and NIR cell imaging reagent. In Fig. 4a, TQ/CB[8], HACD, and SR101 were defined as the “input”, and the signal intensity of the phosphorescent supramolecular at 550 nm was defined as the “output” signal. The phosphorescence peak intensity higher than 200 k was defined as “1”, and lower than this value was set as “0”. After adding the acceptor dye SR101, the phosphorescence signal of the assembly TQ/CB[8]/HACD decreased. Thus, SR101 dye can be used as the “NOT” gate, and its addition can make the phosphorescence system output a “silent” mode. Therefore, the hierarchical confinement achieving supramolecular phosphorescence logic gate could output more complex and reliable information. Furthermore, we also investigated the cell imaging possibility of water-soluble NIR fluorescence supramolecule. After incubation with 293T cells, it gives a cell survival rate of up to 89.2% (Fig. S20 in Supporting information), showing satisfactory biosafety. Furthermore, the dialysis experiments of the NIR supramolecule under physiological conditions demonstrated no detectable SR101, Cy5, or TQ presence in the external solution of the dialysis membrane by UV-vis spectroscopy (Fig. S21 in Supporting information), excluding the leakage of dyes from assembly. Thus, the fabricated NIR supramolecule is suitable for cancer cell imaging. In cell imaging experiments, the red fluorescence signal was observed in Figure 4b I, manifesting that the supramolecule enters the cancer cells after 24 h of incubation with the HeLa

cells. In addition, both the green lysosomal marker dye (Fig. 4b II) and mitochondrial probe (Fig. S22 in Supporting information) could not be colocalized with the red supramolecule (merged pictures in Fig. 4b III and Fig. S16). Interestingly, the purple signal was found in the merged images (Fig. 4b V) of the NIR supramolecule (Fig. 4b I) and the blue nuclei dye DAPI (Fig. 4b IV), indicating that the NIR supramolecular assembly can selectively enter the cell nuclei, showing targeted ability for the nucleus.

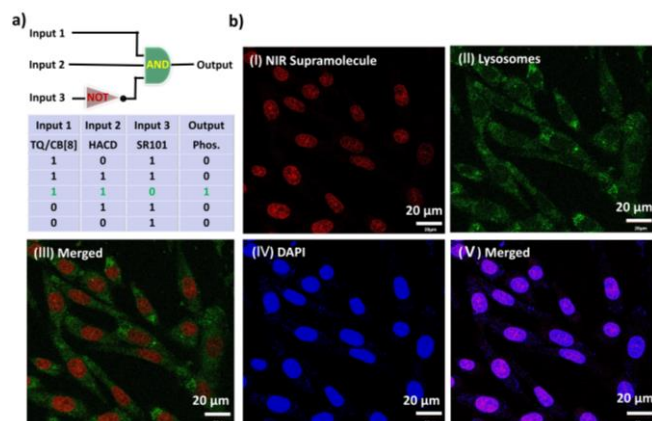


Fig. 4. (a) Supramolecular phosphorescence logic gate. (b) Confocal microscopy images of HeLa cells in the presence of (I) NIR supramolecule TQ/CB[8]/HACD/SR101/Cy5, (II) lysosomal marker dyes, (III) the merged pictures of (I) and (II); (IV) DAPI, (V) the merged pictures of (I) and (IV), respectively ([TQ] = 0.1 mmol/L, [CB[8]] = 0.2 mmol/L, [HACD] = 0.06 mmol/L, [SR101] = 0.005 mmol/L, [Cy5] = 0.001 mmol/L).

In conclusion, the hierarchical confinement strategy not only successfully realizes the activation and enhancement of 3D SOF phosphorescence in the aqueous, but also regulates the assembly morphology from nanoblocks to nanoparticles. Moreover, the phosphorescent supramolecule can effectively encapsulate the dyes SR101 and Cy5 to form a cascade energy-transfer supramolecular system, realizing the regulation of emission peak wavelength and lifetime, especially achieving the secondary energy transfer processes to give long-lived NIR luminescence. This supramolecular system was successfully applied in phosphorescence logic gates and targeted NIR cell imaging for the nucleus.

Declaration of competing interest

The authors report no declarations of interest.

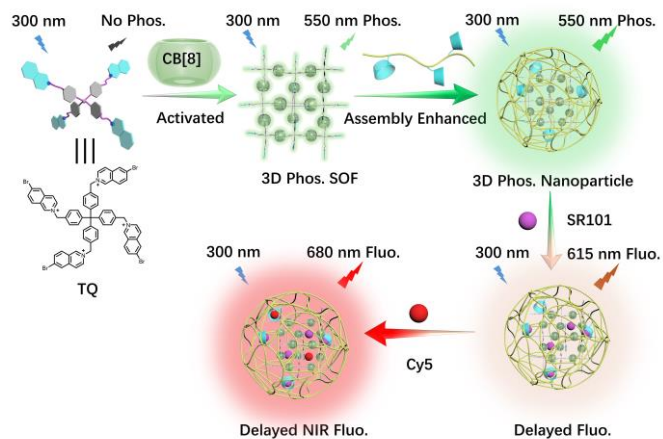
Acknowledgment

This work was financially supported by the National Natural Science Foundation of China (No. 22201142).

References

- [1] X. Wang, C. Chen, Y. Tian, Q.W. Zhang, *J. Am. Chem. Soc.* 147 (2025) 17994-18002.
- [2] W. Feng, F. Li, Z. Jiang, et al., *Angew. Chem. Int. Ed.* 64 (2025) e2025092.
- [3] Q. Niu, Y. Zhang, Z. Ge, et al., *Chin. Chem. Lett.* 36 (2025) 110935.
- [4] Z.Y. Zhang, C.Y. Deng, C.C. Shen, et al., *Chem. Commun.* 59 (2023) 11248-11251.
- [5] J. Yu, H. Wang, Y. Liu, *Adv. Opt. Mater.* 10 (2022) 2201761.

- [6] H. Masai, M. Liu, Y. Tachibana, S. Tsuda, J. Terao, *J. Org. Chem.* 85 (2020) 3082-3091.
- [7] D. Hoenders, S. Ludwanowski, C. Barner-Kowollik, A. Walther, *Angew. Chem. Int. Ed.* 63 (2024) e202405582.
- [8] K. I. Assaf, W. M. Nau, *Acc. Chem. Res.* 56 (2023) 3451-3461.
- [9] A. McLean, R. L. Sala, B. W. Longbottom, et al., *J. Am. Chem. Soc.* 146 (2024) 12877-12882.
- [10] S. Garain, B. C. Garain, M. Eswaramoorthy, S. K. Pati, S. J. George, *Angew. Chem. Int. Ed.* 60 (2021) 19720-19724.
- [11] D. Li, Z. Liu, M. Fang, et al., *ACS Nano* 17 (2023) 12895-12902.
- [12] H.J. Yu, Q. Zhou, X. Dai, et al., *J. Am. Chem. Soc.* 143 (2021) 13887-13894.
- [13] F. Lin, S.B. Yu, Y.Y. Liu, et al., *Adv. Mater.* 34 (2022) 2200549.
- [14] S.-B. Yu, F. Lin, J. Tian, et al., *Chem. Soc. Rev.* 51 (2022) 434-449.
- [15] X. Yao, N. Han, H. Liu, L. Xing, *Chin. Chem. Lett.* (2025) doi.org/10.1016/j.ccllet.2025.111426.
- [16] C. Yan, Q. Li, X. Miao, et al., *Angew. Chem. Int. Ed.* 62 (2023) e202308029.
- [17] C. Yin, Z.A. Yan, R. Yan, et al., *Adv. Funct. Mater.* 34 (2024) 202316008.
- [18] J. Yu, J. Niu, X. Xu, Y. Liu, *Adv. Sci.* 11 (2024) 2408107.
- [19] X. Chen, H. K. Bisoyi, X.F. Chen, et al., *Matter* 5 (2022) 3883-3900.
- [20] Y. Li, Q. Li, X. Miao, et al., *Angew. Chem. Int. Ed.* 60 (2021) 6744-6751.
- [21] J. Rühle, K. Vinod, H. Hoh, et al., *J. Am. Chem. Soc.* 146 (2024) 28222-28232.
- [22] S. Garain, P.L. Li, K. Shoyama, F. Würthner, *Angew. Chem. Int. Ed.* 63 (2024) e202411102.
- [23] P. Jiang, B. Ding, T. Li, et al., *Sci. China Chem.* 68 (2025) 2533-2540.
- [24] M. Wang, X. Liu, W. Yuan, et al., *Adv. Mater.* 37 (2025) 2415446.
- [25] T. Kim, H. S. Han, K. Yang, et al., *ACS Nano* 18 (2024) 7972-7988.
- [26] C. Sun, Z. Wang, L. Yue, et al., *J. Am. Chem. Soc.* 142 (2020) 16523-16527.
- [27] Y. Zhang, L. Wang, J. Wang, S. Xin, X. Sheng, *Chin. Chem. Lett.* 32 (2021) 1902-1906.



Multiscale hierarchical confinement of macrocyclic and assembly can not only effectively activate and improve the phosphorescence performance of the SOF but also regulate the supramolecular morphology, boosting efficient cascade phosphorescence resonance energy transfer to achieve NIR emission in water, which was successfully applied in phosphorescence logic gate and targeted cell imaging.

Graphical abstract

Declaration of Interest Statement

The authors declare that they have no known competing financial interests or personal relationships that could have appeared to influence the work reported in this paper.

The author is an Editorial Board Member/Editor-in-Chief/Associate Editor/Guest Editor for this journal and was not involved in the editorial review or the decision to publish this article.

The authors declare the following financial interests/personal relationships which may be considered as potential competing interests: